Published in final edited form as:
J Immunol. 2011 December 15; 187(12): 6374–6381. doi:10.4049/jimmunol.1102611.

Regulation of T cell receptor β allelic exclusion by gene segment proximity and accessibility[1,,2]

Hrisavgi D. Kondilis-Mangum[*], **Han-Yu Shih**[*], **Grace Mahowald**[+], **Barry P. Sleckman**[+], and **Michael S. Krangel**[*]

[*]Department of Immunology, Duke University Medical Center, Durham NC 27710

[+]Department of Pathology and Immunology, Washington University School of Medicine, St. Louis, Missouri 63110

Abstract

Antigen receptor loci are regulated to promote allelic exclusion, but the mechanisms are not well understood. Assembly of a functional T cell receptor (TCR) β chain gene triggers feedback inhibition of V_β-to-DJ_β recombination in double positive (DP) thymocytes which correlates with reduced V_β chromatin accessibility and a locus conformational change that separates V_β from DJ_β gene segments. We previously generated a *Tcrb* allele that maintained V_β accessibility but was still subject to feedback inhibiton in DP thymocytes. We have now further analyzed the contributions of chromatin accessibility and locus conformation to feedback inhibition using two novel TCR alleles. We show that reduced V_β accessibility and increased distance between V_β and DJ_β gene segments both enforce feedback inhibition in DP thymocytes.

Introduction

A defining characteristic of T- and B-lymphocytes is their ability to create and express unique antigen receptors that can recognize a vast array of foreign pathogens. To achieve receptor diversity, antigen receptor variable domains are encoded by multiple variable (V), diversity (D), and joining (J) gene segments that are joined by a process known as V(D)J recombination (1). Recombination Activating Genes 1 and 2 (RAG1/2) mediate V(D)J recombination by: (i) binding to recombination signal sequences (RSSs)[3] that flank antigen receptor gene segments, (ii) bringing two RSSs (one with a 12 and one with a 23 bp spacer) into a synaptic complex, and (iii) generating DNA double strand breaks between the coding sequences and RSSs. Hairpin-sealed coding ends are subsequently opened by the Artemis endonuclease and ligated by non-homologous end joining proteins to form antigen receptor coding joints. Because RAG1/2-generated double strand breaks are potentially toxic, V(D)J recombination is highly regulated.

B cell receptor and T cell receptor (TCR) genes undergo stepwise recombination in developing B and T lymphocytes, respectively (2–4). *Igh* rearranges in pro-B cells and *Igk* and *Igl* rearrange in pre-B cells; *Tcrb*, *Tcrg* and *Tcrd* rearrange in $CD4^-CD8^-$ double negative (DN) thymocytes and *Tcra* rearranges in $CD4^+CD8^+$ double positive (DP)

[1]This work was supported by National Institutes of Health Grant AI049934 (to M.S.K.).

[2]Address correspondence to: Michael S. Krangel, Department of Immunology, Campus Box 3010, Duke University Medical Center, Durham NC 27710. Tel: 919-684-4985; Fax: 919-684-8982; krang001@mc.duke.edu.

[3]Abbreviations used in this paper: 3D-FISH, three-dimensional fluorescence *in situ* hybridization; DN, double negative; DP, double positive; E_α, *Tcra* enhancer; ES, embryonal stem; H3K4me3; histone H3 lysine 4 trimethylation; LM-PCR, ligation-mediated-polymerase chain reaction; PDβ1, promoter Dβ1; RSS, recombination signal sequence; SE, signal end; tg, transgene.

thymocytes. Moreover, *Igh* and *Tcrb* rearrangements are ordered such that D-to-J recombination precedes V-to-DJ recombination. This regulation is achieved, in part, by *cis*-elements such as enhancers and promoters that alter the chromatin landscape to make RSSs accessible to RAG1/2 (5). Accessible chromatin is characterized by active transcription, by histone H3 and H4 acetylation, by histone H3 lysine 4 trimethylation (H3K4me3), by displacement and removal of nucleosomes, and by hypomethylation of CpG dinucleotides (2, 4). H3K4me3-modified nucleosomes also stimulate V(D)J recombination by docking RAG2 (6, 7) and enhancing the catalytic activity of the RAG1/2 complex (8).

Antigen receptor loci also undergo changes in their conformation during lymphocyte development (9). A contracted locus conformation is thought to promote V(D)J recombination by facilitating the interaction between RSSs separated by great distances (e.g. V_β and D_β RSSs, V_H and D_H RSSs). Detailed analysis of contracted *Igh* loci revealed that V_H segments spanning 2.5 megabases are all situated proximal to D_H RSSs, presumably affording them all an opportunity for recombination (10). This interpretation is supported by the behavior of *Pax5* deficient pro B-cells, in which *Igh* contraction and distal V_H recombination are both impaired (11).

Antigen receptor loci are also regulated to enforce allelic exclusion (12–14). For *Igh* and *Tcrb*, allelic exclusion is manifest at the V-to-DJ step and is thought to occur in two phases: 1) an initiation phase, in which V-to-DJ recombination is regulated so that it is not attempted simultaneously on the two alleles, and 2) a maintenance phase, in which V-to-DJ recombination is terminated by a feedback mechanism once an in-frame rearrangement is produced. Feedback inhibition of *Igh* recombination in pre B-cells and of *Tcrb* recombination in DP thymocytes is associated with epigenetic and locus conformational changes. Thus, whereas *Igh* and *Tcrb* alleles are by multiple criteria accessible in pro-B cells and DN thymocytes, respectively, their V gene segments display reduced accessibility in pre-B cells and DP thymocytes (2, 13, 14). In addition, unrearranged *Igh* and *Tcrb* alleles, while contracted in pro-B and DN thymocytes, respectively, become decontracted in pre B-cells and DP thymocytes (15, 16). These changes could inhibit recombination by limiting RAG1/2 binding to V segment RSSs and the likelihood of RSS synapsis.

Several genetically modified *Igh* and *Tcrb* alleles have been created to assess the significance of these changes for feedback inhibition. Two *Tcrb* alleles with large deletions (β^{LD} and $V_\beta1$ NT) (17, 18) moved the otherwise distant $V_\beta10$ gene segment into proximity of DJ_β gene segments and increased its accessibility in DP thymocytes. Disruption of allelic exclusion was detected on $V_\beta1$ NT alleles only, but no data evaluated whether altered $V_\beta10$ recombination reflected a loss of feedback inhibition in DP thymocytes as opposed to dysregulated rearrangement in DN thymocytes. Another study simply inserted a V_β gene segment just upstream of DJ_β gene segments (19). While allelic exclusion was perturbed at the level of V_β recombination, whether this reflected a loss of feedback inhibition in DP thymocytes was not evaluated in this study either. Bates *et al.* generated a modified *Igh* allele in which a V_H gene segment was introduced just upstream of D_H gene segments (20). This allele clearly displayed a disruption of feedback inhibition in pre-B cells. However, as the genetic manipulation moved the V_H into an accessible chromatin domain and also modulated distance, the individual effects of accessibility and distance could not be distinguished.

Jackson *et al.* previously generated a *Tcrb* allele in which V_β accessibility was maintained in DP thymocytes by introducing the *Tcra* enhancer (E_α) into the middle of the V_β array (EαKI allele) (21). Despite accessible V_β chromatin, feedback inhibition of V_β-to-DJ_β recombination was maintained in DP thymocytes, indicating that parameters other than chromatin accessibility must be essential to enforce feedback inhibition in DP thymocytes.

We have now further analyzed contributions of gene segment accessibility and proximity to feedback inhibition through the generation of two novel TCR alleles. Our results establish that reduced RSS accessibility and increased distance between RSSs both contribute to feedback inhibition of V_β-to-DJ_β recombination in DP thymocytes.

Materials and Methods

Mice and gene targeting

Wild-type 129, *Rag2*$^{-/-}$ (22) and *Rag2*$^{-/-}$ mice containing a rearranged *Tcrb* tg (23) were purchased from Taconic. EαKI, EαKI *Rag2*$^{-/-}$, and EαKI *Rag2*$^{-/-}$ *Tcrb* tg mice were previously described (21). All mice were used in accordance with protocols approved by the Duke University and Washington University Animal Care and Use Committees.

DJEαKI mice were generated as follows: DJ_βKI and homology arms were PCR amplified using Pfu Turbo (Stratagene) and cloned using a TOPO Cloning kit (Invitrogen, Carlsbad, CA). DJ_βKI was PCR amplified from a plasmid carrying $PD_\beta1$ and a $D_\beta1$-$J_\beta1.1$ rearrangement (5′ end at nucleotide 152528 and 3′ end at nucleotide 154066 of Genbank file MMAE000665). 5′ and 3′ homology arms extended from nucleotides 2531 to 8110 and nucleotides 8115 to 12960 of Genbank file MMAE000664. We introduced a *BamH*I site 90 bp 3′ of the $V_\beta13$ RSS at nucleotide 7425. Cloned fragments were introduced into the pLNTK vector containing a phosphoglycerate kinase (PGK) promoter-driven *lox*P flanked neomycin-resistance (*neo*^{r}) cassette and a thymidine kinase selection marker. The 5′ arm and DJ_βKI were cloned into the *XhoI* site and the 3′ arm was cloned into the *Sal*I site. ES cells derived from EαKI mice (21) were used for homologous recombination which was verified by Southern blot of *Sac*I-digested genomic DNA analyzed with a 5′ *Tcrb* probe and of *EcoR*I-digested genomic DNA analyzed with a 3′ *Tcrb* probe (Supplementary Table 1). The *neo*^{r} cassette was removed by transient transfection of ES cells with *Cre* recombinase.

β-in-α mice were generated as follows: The *Tcrb* substrate was amplified from the DJEαKI targeting construct and extends from nucleotide 5794 of GenBank file MMAE000664 (upstream of the $V_\beta13$ promoter) to nucleotide 154066 of GenBank file MMAE000665 (downstream of $J_\beta1.1$). 5′ and 3′ homology arms extended from nucleotides 12960 to 18291 and 84861 to 87477 of GenBank file M64239. Homology arms and the *Tcrb* substrate were cloned into PGKneolox2.DTA (http://www.addgene.org/pgvec1?f=c&identifier=13449&cmd=findpl&attag=c). The 5′ arm and *Tcrb* substrate were cloned between the *Not*I and *Xma*I sites. The 3′ arm was cloned between the *Nhe*I and the *Sal*I sites. ES cells derived from TCRα^{sJ}/TCRα^{sJ} mice (24) were used for homologous recombination, which was verified by Southern blot of *EcoR*I-digested genomic DNA analyzed with a 3′ TCRα (Cα) probe and using *Kpn*I and *BamH*I-digested genomic DNA analyzed with a 5′ TCRα probe (Supplementary Table 1). The *neo*^{r} cassette was removed by transient transfection of ES cells with *Cre* recombinase.

3D-FISH

Bacterial artificial chromosome clones 75P5 (5′*Tcrb* probe) and 203H5 (3′*Tcrb* probe) were directly labeled and used for 3D-FISH as previously described (25). Probe-to-probe distances were calculated as previously described (25). Only nuclei with two distinguishable signals for both alleles were analyzed. Statistical tests were performed using Prism 3.0 (GraphPad Software, Inc.).

Cell sorting

DN3 thymocytes were isolated as previously described (26). Cells were stained with the following antibodies for 30 minutes on ice: Cy5-conjugated anti-CD3ε (clone 145-2C11),

anti-CD4 (clone GK1.5), and anti-CD8 (clone 53-6.7); biotinylated anti-CD24 (clone M1-69), PE-conjugated anti-CD44 (clone 1M7), and FITC-conjugated anti-CD25 (clone 7D4). After washing, cells were stained with Texas Red-conjugated streptavidin. Cells were collected from the $CD24^+CD3^-CD4^-CD8^-$ and $CD25^+CD44^+$ gates. DP thymocytes were isolated as previously described (26). Cells were stained with FITC-conjugated anti-CD4 (clone GK1.5) and PE-conjugated anti-CD8 (clone 53-6.7) for 30 minutes on ice. Cells were collected from the $CD4^+CD8^+$ gate. All antibodies were purchased from eBioscience. Samples were sorted to at least 95% purity using a DiVa cell sorter (Becton Dickinson); analysis was with CellQuest software.

Chromatin immunoprecipitation

Chromatin was prepared from primary thymocytes of 2–3 week old mice by small scale micrococcal nuclease digestion as previously described (27). Immunoprecipitations were performed using anti-H3K4me3 (Millipore, 04–745, clone MC315) and normal rabbit IgG (R&D Systems, AB-105-C). All samples were resuspended in 200 μl of 10 mM Tris-HCl pH 8, 0.1 mM EDTA; input samples were further diluted 1:50. Bound and input samples were quantified using 2 μl of sample by SYBR Green real-time PCR using a LightCycler 480 (Roche). All PCR amplifications used a touchdown strategy (TD-qPCR) in which annealing temperature was reduced gradually from 65°C to 58°C over 10 cycles, followed by 35 cycles at 58°C. Primers used are listed in Supplementary Table 1.

Germline transcription

Approximately 2×10^7 primary thymocytes were resuspended in 1 ml of Trizol (Invitrogen) and RNA was isolated according to manufacturer's instructions. cDNA was synthesized using the Super Script III kit (Invitrogen) using up to 2 μg of purified RNA. Transcripts were quantified by SYBR Green real-time PCR using the TD-qPCR program. *Actb* was amplified for 40 cycles at 62°C. Primers are listed in Supplementary Table 1.

Coding joints

Genomic DNA isolated from sorted DN3 and DP thymocytes was amplified by touchdown PCR (TD-PCR) as follows: 5 minutes at 94°C, 31–35 cycles of 30 seconds at 94°C, 30 seconds at annealing temperature, and 30–60 seconds at 72°C. Annealing temperature was held at 68°C, 66°C and 64°C for 5 cycles each and at 62°C for the remaining cycles. Amplicons were resolved on a 2.0% agarose gel, were transferred onto a nylon membrane, and were detected by hybridization with $\gamma\ ^{32}$P-labeled oligonucleotide probes. *Cd14* was amplified for 23 cycles at 62°C. Primers and probes are listed in Supplementary Table 1.

RSS retention

DP thymocyte genomic DNA was amplified by TD-qPCR as described above. Primers are listed in Supplementary Table 1.

Genomic Southern blot

Whole thymus genomic DNA was digested with restriction enzyme, subjected to 0.7% agarose gel electrophoresis and transferred to a nylon membrane. Blots were hybridized with α^{32}P-labeled probes listed in Supplementary Table 1.

Signal ends

Genomic DNA (1.5 μg) of DN3 and DP thymocytes was analyzed by LM-PCR as previously described (21, 28). Amplification by TD-PCR and detection of amplicons was as described above. Supplementary Table 1 lists linker sequences, primers and probes.

Results

EαKI locus conformation

Previous studies of mice carrying *Tcrb* alleles with an introduced E_α (EαKI; Fig 1A) indicated that elevation of V_β accessibility, by itself, could not subvert feedback inhibition of V_β-to-DJ_β recombination in DP thymocytes. We hypothesized that recombination might remain suppressed on accessible EαKI alleles if, like wild-type alleles, they were decontracted in DP thymocytes. To assess this, we used three-dimensional fluorescence *in situ* hybridization (3D-FISH) to measure the distance between the 5′ and 3′ ends of wild-type and EαKI *Tcrb* alleles in recombinase-deficient DN and DP thymocytes (Fig 2). Consistent with previous experiments (16), we found that, on average, wild-type alleles were contracted in DN thymocytes and decontracted in DP thymocytes. The behavior of EαKI alleles was indistinguishable from wild-type, indicating that they decontract in DP thymocytes despite the presence of E_α and an accessible chromatin configuration. Therefore, to formally test whether the distance between accessible V_β and DJ_β gene segments limited V_β-to-DJ_β recombination in DP thymocytes, we generated and characterized two novel TCR locus alleles that approximated accessible V_β and DJ_β gene segments in DP thymocytes.

Regulation of the DJEαKI allele

We used homologous recombination to introduce a cassette containing the $D_\beta1$ promoter ($PD_\beta1$) and a rearranged $D_\beta1J_\beta1.1$ (DJ_βKI) approximately 1.0 kb 3′ of the $V_\beta13$ RSS on the EαKI allele (DJEαKI allele; Fig 1A). Mice homozygous for the DJEαKI allele displayed normal thymocyte development as assessed by cell number and expression of cell surface markers CD4, CD8, CD25 and CD44 (data not shown).

We addressed chromatin accessibility on the DJEαKI allele by introducing it onto *Rag2*-deficient (*Rag2*$^{-/-}$) and *Rag2*$^{-/-}$ x*Tcrb* transgene (tg) backgrounds for analysis of steady state germline transcripts and histone modifications in DN and DP thymocytes. Like $D_\beta1$ transcripts on wild-type alleles, DJ_βKI transcripts on DJEαKI alleles were of comparable abundance in DN and DP thymocytes (Fig 3A, right). Moreover, like nucleosomes at the $D_\beta1$ RSS on wild-type alleles, those at the DJ_βKI RSS on DJEαKI alleles were H3K4me3-modified in DN thymocytes and displayed increased H3K4me3 in DP thymocytes (Fig 3B, right). Hence, the DJ_βKI RSS appears to reside in accessible chromatin in both DN and DP thymocytes of DJ EαKI mice.

As documented previously (21), germline transcription of $V_\beta13$ is downregulated on transition from DN to DP on wild-type alleles but is upregulated on EαKI alleles (Fig 3A, middle). Unexpectedly, we found that introduction of the DJ_βKI blunted the effect of E_α on $V_\beta13$ in DJEαKI DP thymocytes, such that $V_\beta13$ transcripts were upregulated as compared to wild-type DP thymocytes, but were no more abundant in DJEαKI DP than in DJEαKI DN thymocytes. This might reflect a suppression of transcription due to competition between $PD_\beta1$ and the $V_\beta13$ promoter, or an effect of the DJ_βKI on $V_\beta13$ transcript stability. The DJ_βKI also unexpectedly suppressed H3K4me3 at the $V_\beta13$ RSS in both DN and DP thymocytes (Fig. 3B, center). Given these results, we also analyzed accessibility at $V_\beta8.1$, which lies 5 kb upstream of $V_\beta13$. Unlike $V_\beta13$, the upregulation of $V_\beta8.1$ transcription in EαKI DP thymocytes was maintained in DJEαKI DP thymocytes (Fig. 3A, left). Moreover, the upregulation of $V_\beta8.1$ H3K4me3 in EαKI DP thymocytes was only partly suppressed by the DJ_βKI (Fig. 3B, left). Taken together, the transcription and chromatin data suggest that $V_\beta13$ is moderately accessible and that $V_\beta8.1$ is highly accessible in DJEαKI DN and DP thymocytes.

To analyze V_β-to-DJ_β recombination, we prepared genomic DNA from purified DN3 and DP thymocytes of EαKI and DJEαKI mice, amplified with $V_\beta13$ and $J_\beta1.1$ primers, and

distinguished DJ_βKI from endogenous $DJ_\beta1.1$ rearrangement using a DJ_βKI-specific probe (Fig. 4A). $V_\beta13$-to-DJ_βKI rearrangement was readily detected in sorted DN3 and DP thymocytes of DJEαKI mice but not in EαKI controls. To measure the frequency of DJβKI recombination, we quantified residual unrearranged $V_\beta13$ and DJ_βKI RSSs in DP thymocyte genomic DNA (Fig. 4B, center and right). We found that approximately 70% of the DJ_βKI and $V_\beta13$ RSSs were lost in DJEαKI DP thymocytes. These losses likely reflect recombination to DJ_βKI as well as recombination to the endogenous D_β gene segments that would delete $V_\beta13$ and DJ_βKI.

We also analyzed DJ_βKI recombination by genomic Southern blot of *EcoR*I-digested whole thymus DNA (Fig. 4C). As compared to DJEαKI kidney (lane 2), a $V_\beta13$ probe detected substantial loss of DNA carrying unrearranged $V_\beta13$ and DJ_βKI, and detected two major and several minor rearranged fragments (lane 3). However, the predicted 8.0 kb fragment representing $V_\beta13$-DJ_βKI rearrangement was not detected. The additional rearranged fragments may represent excision circles carrying signal joints generated by rearrangement of upstream V_β segments to DJ_βKI (eg., $V_\beta8.1$ = 6.7 kb, $V_\beta8.2$ = 5.5 kb $V_\beta8.3$ = 3.0 kb, $V_\beta5.1$ = 4.2 kb and, $V_\beta5.2$ = 4.6 kb), as well as DJ_βKI signal end (SE) recombination intermediates (2.5 kb), all of which would hybridize to the $V_\beta13$ probe. Consistent with the former, we detected $V_\beta8.1$-to-DJ_βKI recombination using a PCR strategy (Fig. 4A). Excision circles and SE intermediates generated in DN thymocytes should be undetectable by genomic Southern blot of whole thymus because they would be diluted by the proliferative burst that accompanies the DN to DP transition. The apparent abundance of $V_\beta13$-containing excision circles and DJ_βKI SE intermediates in DJEαKI thymocytes suggested that they were generated by recombination events occurring in DP rather than in DN thymocytes.

To test directly for V_β and DJ_βKI recombination in DP thymocytes, we used ligation-mediated-PCR (LM-PCR) to detect SE recombination intermediates in sorted thymocyte subpopulations (Fig. 4D). Because this assay cannot distinguish DJ_βKI from endogenous $D_\beta1$ SEs, we evaluated DJ_βKI SEs by comparison of DJEαKI to EαKI samples. As expected, 5′ $D_\beta1$, $V_\beta13$ and $V_\beta8.1$ SEs were readily detected in EαKI DN thymocytes but were barely detected in EαKI DP thymocytes. However these SE intermediates were all readily detected in DJEαKI DP thymocytes (Fig. 4D). In contrast, control 5′ $D_\beta2$ SEs were undetectable in DJEαKI DP thymocytes, indicating a selective loss of feedback inhibition involving DJ_βKI and upstream V_β gene segments.

To formally demonstrate that DJ_βKI rearrangements in DP thymocytes occurred chromosomally rather than on excision circles generated by V_β-to-endogenous D_β recombination in DN thymocytes, we analyzed V_β-to-DJ_βKI recombination in thymocytes of DJEαKI mice that express a *Tcrb* tg. Feedback inhibition by such transgenes specifically suppresses V_β-to-DJ_β recombination and the excision circles generated by these recombination events (21). Indeed, increased retention of a DNA segment situated 5′ of $D_\beta1$, normally lost during V_β-to-endogenous DJ_β recombination, was apparent in wild-type, EαKI and DJEαKI *Tcrb* tg DP thymocytes (Fig. 4B, left). However, suppression of $V_\beta13$ and DJ_βKI RSS loss was only partial in DJEαKI *Tcrb* tg DP thymocytes and for $V_\beta13$ was much diminished as compared to the complete suppression in EaKI *Tcrb* tg DP thymocytes (Fig. 4B, center and right). This indicates continued chromosomal recombination of $V_\beta13$ and upstream V_βs to DJ_βKI in DP thymocytes, despite feedback inhibition of endogenous V_β-to-DJ_β recombination by the *Tcrb* tg. Consistent with this interpretation, recombination events detected by the $V_\beta13$ probe were more abundant on Southern blots of DJEαKI *Tcrb* tg thymus DNA (Fig. 4C, compare lanes 3 and 4) and $V_\beta13$ and DJ_βKI SE intermediates were more abundant in DJEαKI *Tcrb* tg thymus DNA (Fig. 4D). We conclude that by reducing

the distance between accessible gene segments, the DJ_βKI promotes chromosomal V_β recombination in DP thymocytes and thereby subverts the process of feedback inhibition.

Regulation of theβ-in-α allele

To further assess constraints on *Tcrb* gene segment recombination in DP thymocytes, we introduced a *Tcrb* recombination substrate into the *Tcra* locus, since this locus normally undergoes recombination in DP thymocytes (*Tcrb*-in-*Tcra*; β-in-α allele). The *Tcrb* substrate contained the same DJ_βKI as in the DJEαKI allele, with the V_β13 promoter and gene segment (V_β13KI) situated just upstream (Fig. 1B). A *BamH*I site introduced approximately 90 bp 3′ of the V_β13 RSS was used in some experiments to distinguish the V_β13KI from the endogenous V_β13. We used homologous recombination to introduce this *Tcrb* recombination substrate into a previously generated *Tcra* allele ($TCR\alpha^{sJ}$, which contains only the J_α61 and J_α56 gene segments (24)), such that it replaces the TEA promoter and the entire J_α array of the wild-type *Tcra* locus. In this way, the *Tcrb* recombination substrate carries V_β and DJ_β segments that are in close physical proximity and that will be accessible in DP thymocytes due to the activity of the endogenous E_α. We generated heterozygous β-in-α mice which were then intercrossed to produce β-in-α homozygous mice (Fig. 1B). These mice displayed normal DN thymocyte development and efficient differentiation to the DP stage, but were blocked in their development beyond the DP stage (data not shown). We presume that the chimeric TCRα proteins encoded by β-in-α alleles (which would include D_β and J_β, rather than J_α sequences) are either unstable, cannot assemble with TCRβ proteins, or cannot create a TCRαβ complex that can support positive selection.

We analyzed germline transcription and H3K4me3 modified nucleosomes on the β-in-α allele after introducing it onto *Rag2*$^{-/-}$ and *Rag2*$^{-/-}$ x*Tcrb* tg backgrounds. As expected, transcription of the DJ_βKI was low in DN thymocytes and was substantially upregulated in DP thymocytes (Fig. 5A, left). Specific amplification of V_β13KI revealed it to behave similarly (Fig. 5A, center). We also directly compared V_β13KI transcription to endogenous V_β13 transcription using a PCR strategy that amplified both equally (Fig. 5B, right). V_β13KI transcripts were more abundant in β-in-α DP thymocytes than were endogenous V_β13 transcripts in wild-type DN thymocytes. Similar conclusions were drawn from analysis of H3K4me3 on β-in-α alleles (Fig. 5B). These data suggest that the *Tcrb* substrate, like J_α gene segments on a wild-type allele, is regulated by E_α and is highly accessible in β-in-α DP thymocytes.

We assayed V_β13KI-to-DJ_βKI recombination in wild-type and β-in-α DN3 and DP thymocytes by amplification with V_β13 and J_β1.1 primers followed by hybridization with a DJ_βKI-specific probe (Fig. 6A). This strategy detected the germline (G) substrate in βin-α DN and DP thymocytes (Fig. 6A), but detected abundant V_β13KI-to-DJ_βKI rearranged (R) alleles selectively in β-in-α DP thymocytes (Fig. 6A). On the basis of germline RSS loss, fully 60% of the DJ_βKI had undergone recombination in β-in-α DP thymocytes (Fig. 6B). However, the same analysis indicated that only about 10% of the V_β13 KI had undergone recombination (Fig. 6B), indicating that DJ_βKI could rearrange to RSSs other than V_β13 KI. To further address this, we hybridized *Eco*RI-digested whole thymus genomic DNA to V_β13 and C_α probes. In addition to unrearranged V_β13 (7.8 kb) and unrearranged V_β13KI (5.9 kb), the V_β13 probe detected a potential DJ_βKI SE intermediate (2.5 kb) and one or two additional minor species (Fig. 6C, lane 3). However, consistent with low frequency V_β13KI recombination, we could not detect V_β13KI-to-DJ_βKI rearranged alleles (4.3 kb) (Fig 6C, lane 3). The C_α probe also detected a 5.9 kb unrearranged fragment, but in addition detected a large number of additional recombination events involving the DJ_βKI, including a potential 4.3 kb V_β13KI-to-DJ_βKI rearrangement (Fig. 6C, lane 6). However, the majority of DJ_βKI rearrangements did not involve V_β13KI, but presumably, upstream V_α gene segments instead. Thus, V_α RSSs appear to outcompete the V_β13KI RSS for the DJ_βKI RSS *in vivo*.

This result is consistent with previous studies demonstrating that proximal V_α segments are contracted and accessible in DP thymocytes (25, 29), and that V_α RSSs are generally superior to V_β RSSs as recombinase substrates (30).

To confirm that β-in-α alleles undergo recombination and are not subject to feedback inhibition in DP thymocytes, we sorted DN and DP thymocytes from wild-type and β-in-α mice and detected SE recombination intermediates by LM-PCR (Fig. 6D). As previously described (21), wild-type thymocytes displayed $5'D_\beta1$, $5'D_\beta2$ and $V_\beta13$ SEs that were abundant in DN but not in DP thymocytes. In contrast, $5'D_\beta1$ and $V_\beta13$ SEs were at least as abundant in β-in-α DP thymocytes as they were in β-in-α DN thymocytes (Fig. 6D). This represents dysregulation of the β-in-α substrate rather than the endogenous gene segments because $5'D_\beta2$ SEs were reduced in abundance in DP as compared to DN thymocytes. We conclude that β-in-α alleles undergo both $V_\beta13$KI-to-DJ_βKI and endogenous V_α-to-DJ_βKI recombination in DP thymocytes.

Discussion

Numerous studies have correlated reduced antigen receptor locus accessibility and an extended antigen receptor locus conformation with the feedback inhibition of V(D)J recombination that mediates allelic exclusion (2, 13, 14). We previously forced V_β accessibility in DP thymocytes but could not overcome the inhibition of V_β-to-DJ_β recombination that normally characterizes this compartment (21). Here we found that, like wild-type alleles, those accessible EαKI alleles are extended in DP thymocytes. We therefore generated two new alleles (DJEαKI and β-in-α) to formally test whether gene segment proximity and accessibility are both critical effectors of feedback inhibition. By comparing the behavior of DJEαKI to EαKI alleles, we varied the proximity of accessible V_β and DJ_β segments; in DP thymocytes these gene segments are accessible on both alleles, but they are in physical proximity on DJEαKI alleles only. We found that DJEαKI but not EαKI alleles supported V_β-to-DJ_β recombination in DP thymocytes. By comparing β-in-α alleles in DN and DP thymocytes, we varied the accessibility of proximal V_β and DJ_β segments; these gene segments are in physical proximity in both compartments, but become accessible due to developmental activation of E_α in DP thymocytes only. We found that β-in-α alleles supported V_β-to-DJ_β recombination in DP but not in DN thymocytes. Based on the data from both models, we conclude that gene segment accessibility and gene segment proximity are both essential for chromosomal V(D)J recombination, and that feedback inhibition of V_β-to-DJ_β recombination on wild-type *Tcrb* alleles in DP thymocytes is normally enforced by both a loss of RSS accessibility to RAG1/2 and a decontracted locus conformation that inhibits RSS synapsis.

Pre-TCR signals initiate feedback inhibition and promote *Tcrb* epigenetic changes that enforce feedback inhibition, but the critical signaling pathways and downstream effector proteins are only partially understood (14). To the best of our knowledge, the only signaling pathway or downstream effector that has clearly been shown to impact *Tcrb* allelic exclusion through effects in DP thymocytes is the transcription factor E47. E47 supports *Tcrb* locus accessibility and recombination in DN thymocytes and is downregulated in response to pre-TCR signaling in DP thymocytes (31). Notably, its overexpression was shown to override feedback inhibition and to promote V_β-to-DJ_β recombination in DP thymocytes (31). However, *Tcrb* locus accessibility and conformation were not evaluated in E47-overexpressing DP thymocytes, leaving the basis for this override of feedback inhibition undefined. We predict that E47 must support V_β accessibility and *Tcrb* locus contraction to account for the described effects on *Tcrb* recombination.

Although modulation of gene segment proximity appears to represent an important component of the feedback inhibition program, the mechanisms of locus contraction and decontraction are poorly understood. Recent studies have implicated architectural proteins cohesin and CTCF as regulators of long-distance interactions and V(D)J recombination at the *Tcra* and *Igh* loci (32–34) but it is not known whether these proteins regulate overall locus conformation. Eμ (35) and transcription factors Pax5 (11, 36), YY1(37) and Ikaros (38) have all been implicated in *Igh* locus contraction, but whether and how they might trigger *Igh* locus decontraction is uncertain. Much less is known about the roles of architectural proteins and transcriptional regulators in *Tcrb* locus contraction and decontraction events. This will certainly be an important avenue for future studies.

Our data argue that gene segment proximity and accessibility are critical determinants of the *Tcrb* locus feedback inhibition program. Moreover, our results suggest that there are not likely any additional constraints imposed on the rearrangement of most V_β gene segments to $D_\beta 1$ in DP thymocytes, for example, specific factors that regulate the usage of V_β and $5'D_\beta 1$ RSSs. Were such constraints to exist, they should have been unperturbed by our genetic manipulations, and feedback would have remained intact on both the DJEαKI and β-in-α alleles. We caution that we cannot formally eliminate the possibility that what we interpret to result from a change in physical distance could actually reflect the loss of an intervening regulatory element that is intrinsically inhibitory to V_β-to-DJ_β recombination. The identity of that element would be a matter of speculation. However we imagine that it would function, like a change in physical proximity, to limit synapsis of V_β and $D_\beta 1$ RSSs.

Despite the conclusions outlined above, additional layers of regulation may be required to explain the suppression of certain types of *Tcrb* locus recombination events in DP thymocytes. A particularly vexing issue is $V_\beta 14$-to-DJ_β recombination, since, unlike all other V_β gene segments, $V_\beta 14$ is located near D_β and J_β gene segments and its accessibility is not downregulated by pre-TCR signaling and is apparently high in DP thymocytes (17, 39–41). Since D_β and J_β segments are also accessible and support RAG1/2 binding in DP thymocytes (42), the suppression of $V_\beta 14$ rearrangement may depend on unique features of inversional rearrangement (40) or of the $V_\beta 14$ RSS (41).

A second issue is the problem of secondary rearrangements. Reduced accessibility and locus decontraction can account for inhibition of V_β-to-$DJ_\beta 1$ or -$DJ_\beta 2$ rearrangement on a *Tcrb* allele that had not yet undergone V_β rearrangement. However, because the V_β segments immediately upstream of a rearranged V_β are accessible in DP thymocytes (43, 44) and are proximal to accessible downstream $D_\beta 2$ and $J_\beta 2$ segments (42) it is not clear what would suppress secondary V_β-to-$DJ_\beta 2$ rearrangement on an allele that had already undergone primary V_β-to-$DJ_\beta 1$ rearrangement. Recent work has demonstrated that secondary rearrangements can occur on these alleles, and that they can replace even an in-frame $VDJ_\beta 1$ rearrangement (18), but there was no indication that this occurred in DP as opposed to DN thymocytes. Indeed, analysis of DP thymocytes failed to detect SE intermediates at the accessible V_β segments upstream of a rearranged V_β gene segment (43). Moreover, SEs at $5'D_\beta 2$ RSS are strongly suppressed in DP thymocytes (21) (and this study). Thus, DP thymocytes appear not to be permissive for secondary *Tcrb* recombination.

Because we found that accessible V_βs can rearrange to the DJ_βKI in DJEαKI DP thymocytes, it seems unlikely that any additional mechanism that might be required to suppress secondary recombination would be directed at V_β RSSs. However, it remains possible that there is a specific regulatory mechanism directed at the $5'D_\beta 2$ RSS. Indeed, $D_\beta 2$ regulation appears to be unusually complex, with promoters both upstream and downstream of $D_\beta 2$ (45, 46). The downstream promoter is preferentially active on unrearranged alleles and presumably directs $D_\beta 2$-to-$J_\beta 2$ rearrangement; the upstream

promoter only becomes active once the downstream promoter is eliminated by $D_\beta 2$-to-$J_\beta 2$ rearrangement and is likely important to direct V_β-to-$DJ_\beta 2$ rearrangement. Activity of the 5′ promoter suggests that the 5′$D_\beta 2$ RSS resides in accessible chromatin on $D_\beta 2$-to-$J_\beta 2$ rearranged alleles in DP thymocytes. However, it is unclear whether these alleles support RAG1/2 binding, since the only assays of RAG1/2 binding at $D_\beta 2$ in DP thymocytes were conducted on alleles that were in germline configuration and in which only the downstream promoter should have been active (42). Therefore it is not known whether RAG1/2 can bind to the 5′$D_\beta 2$ RSS in DP thymocytes, and it remains possible that secondary rearrangements could be suppressed in DP thymocytes by a specific mechanism that occludes RAG1/2 binding to the 5′$D_\beta 2$ RSS. Our results demonstrate conclusively that, for most V_β gene segments, accessibility and conformational constraints alone can fully account for the suppression of V_β-to-$DJ_\beta 1$ recombination in DP thymocytes. However additional work will be required to clarify the mechanisms, beyond accessibility and conformational constraints, which impart feedback inhibition to $V_\beta 14$ recombination and to secondary recombination events involving $DJ_\beta 2$.

Supplementary Material

Refer to Web version on PubMed Central for supplementary material.

Acknowledgments

We thank L. Martinek of the Duke University Cancer Flow Cytometry Facility for help with cell sorting and analysis; Zanchun Huang for technical assistance; and Dr. Eugene Oltz for critical review of the manuscript.

References

1. Schatz DG, Spanopoulou E. Biochemistry of V(D)J recombination. Curr Top Microbiol Immunol. 2005; 290:49–85. [PubMed: 16480039]
2. Cobb RM, Oestreich KJ, Osipovich OA, Oltz EM. Accessibility control of V(D)J recombination. Adv Immunol. 2006; 91:45–109. [PubMed: 16938538]
3. Krangel MS. Mechanics of T cell receptor gene rearrangement. Curr Opin Immunol. 2009; 21:133–139. [PubMed: 19362456]
4. Schatz DG, Ji Y. Recombination centres and the orchestration of V(D)J recombination. Nat Rev Immunol. 2011; 11:251–263. [PubMed: 21394103]
5. Ji Y, Little AJ, Banerjee JK, Hao B, Oltz EM, Krangel MS, Schatz DG. Promoters, enhancers, and transcription target RAG1 binding during V(D)J recombination. J Exp Med. 2010; 207:2809–2816. [PubMed: 21115692]
6. Matthews AG, Kuo AJ, Ramon-Maiques S, Han S, Champagne KS, Ivanov D, Gallardo M, Carney D, Cheung P, Ciccone DN, Walter KL, Utz PJ, Shi Y, Kutateladze TG, Yang W, Gozani O, Oettinger MA. RAG2 PHD finger couples histone H3 lysine 4 trimethylation with V(D)J recombination. Nature. 2007; 450:1106–1110. [PubMed: 18033247]
7. Liu Y, Subrahmanyam R, Chakraborty T, Sen R, Desiderio S. A plant homeodomain in RAG-2 that binds Hypermethylated lysine 4 of histone H3 is necessary for efficient antigen-receptor-gene rearrangement. Immunity. 2007; 27:561–571. [PubMed: 17936034]
8. Shimazaki N, Tsai AG, Lieber MR. H3K4me3 stimulates the V(D)J RAG complex for both nicking and hairpinning *in trans* in addition to tethering *in cis*: implications for translocations. Mol Cell. 2009; 34:535–544. [PubMed: 19524534]
9. Jhunjhunwala S, van Zelm MC, Peak MM, Murre C. Chromatin architecture and the generation of antigen receptor diversity. Cell. 2009; 138:435–448. [PubMed: 19665968]
10. Jhunjhunwala S, van Zelm MC, Peak MM, Cutchin S, Riblet R, van Dongen JJ, Grosveld FG, Knoch TA, Murre C. The 3D structure of the immunoglobulin heavy-chain locus: implications for long-range genomic interactions. Cell. 2008; 133:265–279. [PubMed: 18423198]

11. Fuxa M, Skok J, Souabni A, Salvagiotto G, Roldan E, Busslinger M. Pax5 induces V-to-DJ rearrangements and locus contraction of the immunoglobulin heavy-chain gene. Genes Dev. 2004; 18:411–422. [PubMed: 15004008]
12. Mostoslavsky R, Alt FW, Rajewsky K. The lingering enigma of the allelic exclusion mechanism. Cell. 2004; 118:539–544. [PubMed: 15339659]
13. Jackson AM, Krangel MS. Turning T-cell receptor β recombination on and off: more questions than answers. Immunol Rev. 2006; 209:129–141. [PubMed: 16448539]
14. Brady BL, Steinel NC, Bassing CH. Antigen receptor allelic exclusion: an update and reappraisal. J Immunol. 2010; 185:3801–3808. [PubMed: 20858891]
15. Roldan E, Fuxa M, Chong W, Martinez D, Novatchkova M, Busslinger M, Skok JA. Locus 'decontraction' and centromeric recruitment contribute to allelic exclusion of the immunoglobulin heavy-chain gene. Nat Immunol. 2005; 6:31–41. [PubMed: 15580273]
16. Skok JA, Gisler R, Novatchkova M, Farmer D, de Laat W, Busslinger M. Reversible contraction by looping of the *Tcra* and *Tcrb* loci in rearranging thymocytes. Nat Immunol. 2007; 8:378–387. [PubMed: 17334367]
17. Senoo M, Wang L, Suzuki D, Takeda N, Shinkai Y, Habu S. Increase of TCR V_β accessibility within E_β regulatory region influences its recombination frequency but not allelic exclusion. J Immunol. 2003; 171:829–835. [PubMed: 12847251]
18. Brady BL, Oropallo MA, Yang-Iott KS, Serwold T, Hochedlinger K, Jaenisch R, Weissman IL, Bassing CH. Position-dependent silencing of germline V_β segments on TCR_β alleles containing preassembled $V_\beta DJ_\beta C_\beta 1$ genes. J Immunol. 2010; 185:3564–3573. [PubMed: 20709953]
19. Sieh P, Chen J. Distinct control of the frequency and allelic exclusion of the V_β gene rearrangement at the TCR β locus. J Immunol. 2001; 167:2121–2129. [PubMed: 11489996]
20. Bates JG, Cado D, Nolla H, Schlissel MS. Chromosomal position of a V_H gene segment determines its activation and inactivation as a substrate for V(D)J recombination. J Exp Med. 2007; 204:3247–3256. [PubMed: 18056289]
21. Jackson A, Kondilis HD, Khor B, Sleckman BP, Krangel MS. Regulation of T cell receptor β allelic exclusion at a level beyond accessibility. Nat Immunol. 2005; 6:189–197. [PubMed: 15640803]
22. Shinkai Y, Rathbun G, Lam KP, Oltz EM, Stewart V, Mendelsohn M, Charron J, Datta M, Young F, Stall AM, et al. RAG-2-deficient mice lack mature lymphocytes owing to inability to initiate V(D)J rearrangement. Cell. 1992; 68:855–867. [PubMed: 1547487]
23. Shinkai Y, Koyasu S, Nakayama K, Murphy KM, Loh DY, Reinherz EL, Alt FW. Restoration of T cell development in RAG-2-deficient mice by functional TCR transgenes. Science. 1993; 259:822–825. [PubMed: 8430336]
24. Huang CY, Sleckman BP, Kanagawa O. Revision of T cell receptor α chain genes is required for normal T lymphocyte development. Proc Natl Acad Sci U S A. 2005; 102:14356–14361. [PubMed: 16186502]
25. Shih HY, Krangel MS. Distinct contracted conformations of the *Tcra/Tcrd* locus during *Tcra* and *Tcrd* recombination. J Exp Med. 2010; 207:1835–1841. [PubMed: 20696701]
26. Roberts JL, Lauzurica P, Krangel MS. Developmental regulation of VDJ recombination by the core fragment of the T cell receptor α enhancer. J Exp Med. 1997; 185:131–140. [PubMed: 8996249]
27. Carabana J, Watanabe A, Hao B, Krangel MS. A barrier-type insulator forms a boundary between active and inactive chromatin at the murine TCRβ locus. J Immunol. 2011; 186:3556–3562. [PubMed: 21317385]
28. McMurry MT, Hernandez-Munain C, Lauzurica P, Krangel MS. Enhancer control of local accessibility to V(D)J recombinase. Mol Cell Biol. 1997; 17:4553–4561. [PubMed: 9234713]
29. Hawwari A, Krangel MS. Regulation of TCR δ and α repertoires by local and long-distance control of variable gene segment chromatin structure. J Exp Med. 2005; 202:467–472. [PubMed: 16087716]
30. Liang HE, Hsu LY, Cado D, Cowell LG, Kelsoe G, Schlissel MS. The "dispensable" portion of RAG2 is necessary for efficient V-to-DJ rearrangement during B and T cell development. Immunity. 2002; 17:639–651. [PubMed: 12433370]

31. Agata Y, Tamaki N, Sakamoto S, Ikawa T, Masuda K, Kawamoto H, Murre C. Regulation of T cell receptor β gene rearrangements and allelic exclusion by the helix-loop-helix protein, E47. Immunity. 2007; 27:871–884. [PubMed: 18093539]
32. Degner SC, Wong TP, Jankevicius G, Feeney AJ. Cutting edge: developmental stage-specific recruitment of cohesin to CTCF sites throughout immunoglobulin loci during B lymphocyte development. J Immunol. 2009; 182:44–48. [PubMed: 19109133]
33. Seitan VC, Hao B, Tachibana-Konwalski K, Lavagnolli T, Mira-Bontenbal H, Brown KE, Teng G, Carroll T, Terry A, Horan K, Marks H, Adams DJ, Schatz DG, Aragon L, Fisher AG, Krangel MS, Nasmyth K, Merkenschlager M. A role for cohesin in T-cell-receptor rearrangement and thymocyte differentiation. Nature. 2011; 476:467–471. [PubMed: 21832993]
34. Guo C, Yoon HS, Franklin A, Jain S, Ebert A, Cheng HL, Hansen E, Despo O, Bossen C, Vettermann C, Bates JG, Richards N, Myers D, Patel H, Gallagher M, Schlissel MS, Murre C, Busslinger M, Giallourakis CC, Alt FW. CTCF-binding elements mediate control of V(D)J recombination. Nature. 2011; 477:424–430. [PubMed: 21909113]
35. Guo C, Gerasimova T, Hao H, Ivanova I, Chakraborty T, Selimyan R, Oltz EM, Sen R. Two Forms of Loops Generate the Chromatin Conformation of the Immunoglobulin Heavy-Chain Gene Locus. Cell. 2011
36. Ebert A, McManus S, Tagoh H, Medvedovic J, Salvagiotto G, Novatchkova M, Tamir I, Sommer A, Jaritz M, Busslinger M. The distal V_H gene cluster of the *Igh* locus contains distinct regulatory elements with Pax5 transcription factor-dependent activity in pro-B cells. Immunity. 2011; 34:175–187. [PubMed: 21349430]
37. Liu H, Schmidt-Supprian M, Shi Y, Hobeika E, Barteneva N, Jumaa H, Pelanda R, Reth M, Skok J, Rajewsky K. Yin Yang 1 is a critical regulator of B-cell development. Genes Dev. 2007; 21:1179–1189. [PubMed: 17504937]
38. Reynaud D I, Demarco A, Reddy KL, Schjerven H, Bertolino E, Chen Z, Smale ST, Winandy S, Singh H. Regulation of B cell fate commitment and immunoglobulin heavy-chain gene rearrangements by Ikaros. Nat Immunol. 2008; 9:927–936. [PubMed: 18568028]
39. Chattopadhyay S, Whitehurst CE, Schwenk F, Chen J. Biochemical and functional analyses of chromatin changes at the TCR-β gene locus during $CD4^-CD8^-$ to $CD4^+CD8^+$ thymocyte differentiation. J Immunol. 1998; 160:1256–1267. [PubMed: 9570542]
40. Mathieu N, Spicuglia S, Gorbatch S, Cabaud O, Fernex C, Verthuy C, Hempel WM, Hueber AO, Ferrier P. Assessing the role of the T cell receptor β gene enhancer in regulating coding joint formation during V(D)J recombination. J Biol Chem. 2003; 278:18101–18109. [PubMed: 12639959]
41. Yang-Iott KS, Carpenter AC, Rowh MA, Steinel N, Brady BL, Hochedlinger K, Jaenisch R, Bassing CH. TCR β feedback signals inhibit the coupling of recombinationally accessible $V_β14$ segments with $DJ_β$ complexes. J Immunol. 2010; 184:1369–1378. [PubMed: 20042591]
42. Ji Y, Resch W, Corbett E, Yamane A, Casellas R, Schatz DG. The *in vivo* pattern of binding of RAG1 and RAG2 to antigen receptor loci. Cell. 2010; 141:419–431. [PubMed: 20398922]
43. Jackson AM, Krangel MS. Allele-specific regulation of TCR β variable gene segment chromatin structure. J Immunol. 2005; 175:5186–5191. [PubMed: 16210623]
44. Jia J, Kondo M, Zhuang Y. Germline transcription from T-cell receptor $V_β$ gene is uncoupled from allelic exclusion. EMBO J. 2007; 26:2387–2399. [PubMed: 17410206]
45. McMillan RE, Sikes ML. Differential activation of dual promoters alters $D_β2$ germline transcription during thymocyte development. J Immunol. 2008; 180:3218–3228. [PubMed: 18292546]
46. McMillan RE, Sikes ML. Promoter activity 5′ of $D_β2$ is coordinated by E47, Runx1, and GATA-3. Mol Immunol. 2009; 46:3009–3017. [PubMed: 19592096]

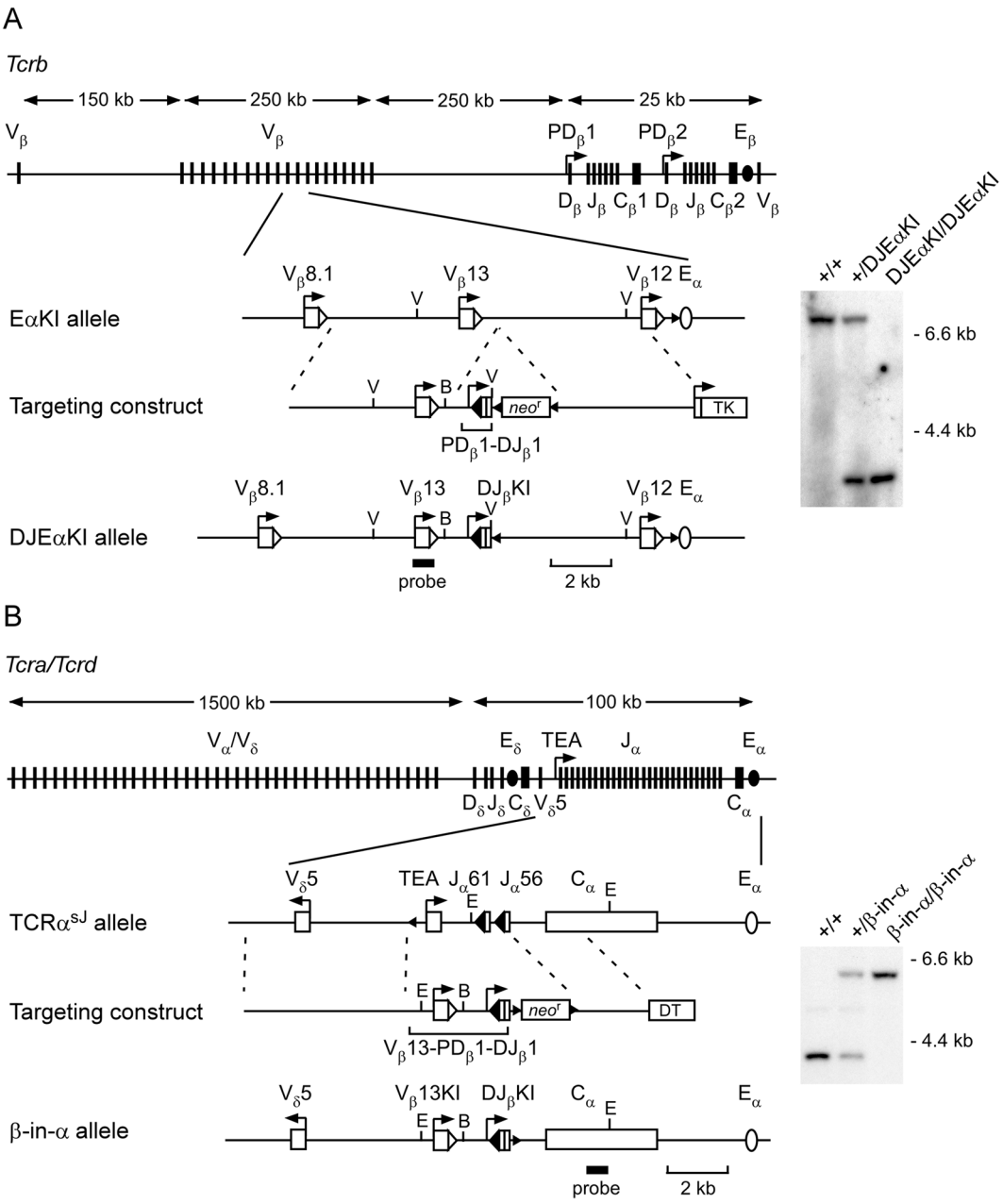

FIGURE 1.

TCR loci and gene targeting strategies. (A) Generation of the DJEαKI allele. Top, *Tcrb* locus, including relative positions of and distances between the V, D, J and C gene segments and *cis*-elements. Below, EαKI allele, targeting construct and DJEαKI allele. Right, Southern blot analysis of genomic DNA from wild-type (+/+), heterozygous (+/DJEαKI) and homozygous (DJEαKI/DJEαKI) mice. DNA was digested with *Eco*RV and hybridized with a V_β13 probe. Expected wild-type and DJEαKI fragments are 7.1 kb and 3.5 kb, respectively. (B) Generation of the β-in-α allele. Top, *Tcra/d* locus, including relative positions of and distances between the V, D, J and C gene segments and *cis*-elements. Below, $TCR\alpha^{sJ}$ allele, targeting construct and β-inα allele. Right, Southern blot of genomic DNA from wild-type (+/+), heterozygous (+/βin-α) and homozygous (β-in-α/β-in-α) mice. DNA was digested with *Eco*RI and hybridized with a 3′ TCRα (C_α) probe. Expected wild-

type and β-in-α fragments are 3.8 kb and 5.9 kb, respectively. V, *Eco*RV; E, *Eco*RI, B, *BamH*I; DT, diphtheria toxin; bent arrow, promoter; open and filled large triangles, 23 bp and 12 bp RSSs, respectively; small triangles, *lox*P sites.

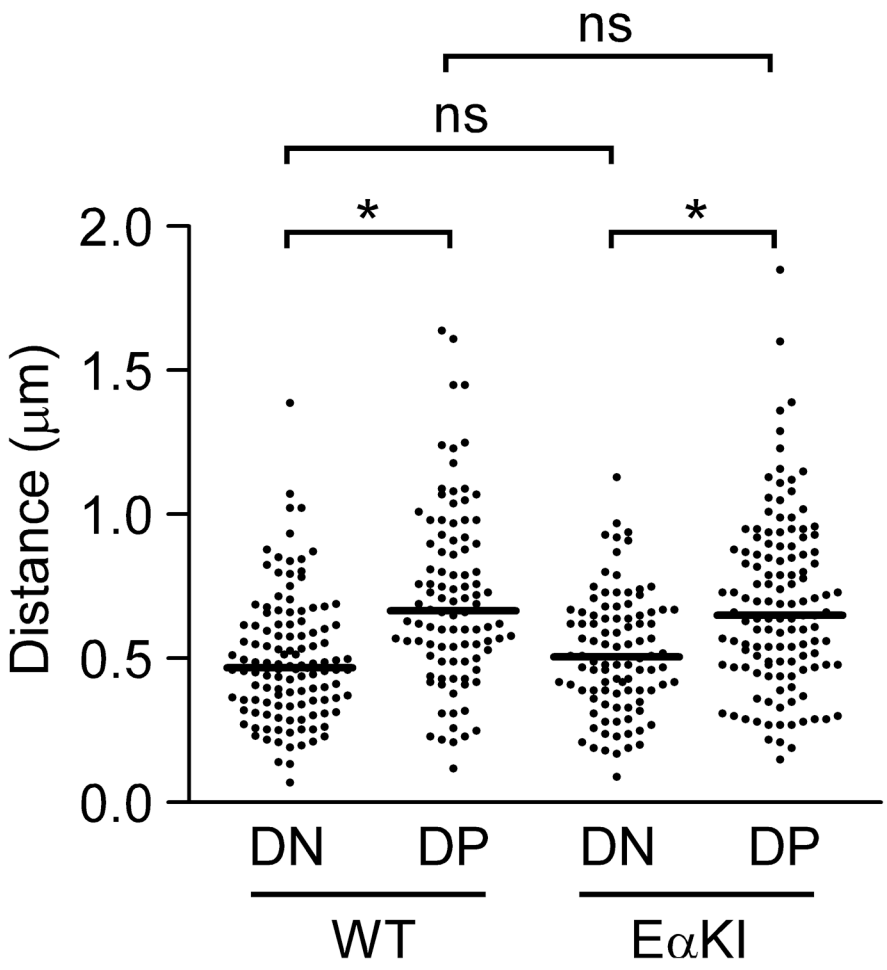

FIGURE 2.

Conformation of wild-type and EαKI alleles. 3D-FISH was performed using probes to the 5′ and 3′ ends of the *Tcrb* locus. Scatter plots display distances between centers of probe hybridization in *Rag2*$^{-/-}$ DN thymocytes (130 alleles from 3 slides), EαKI *Rag2*$^{-/-}$ DN thymocytes (90 alleles from 3 slides), DP thymocytes from *Rag2*$^{-/-}$ mice treated with an anti-CD3ε (90 alleles from 3 slides), and DP thymocytes from EαKI *Rag2*$^{-/-}$ mice treated with anti-CD3ε (130 alleles from 3 slides). Median values are indicated by horizontal lines. *, P<0.0001; ns, not statistically significant. Data were accumulated from two independent experiments for each cell type.

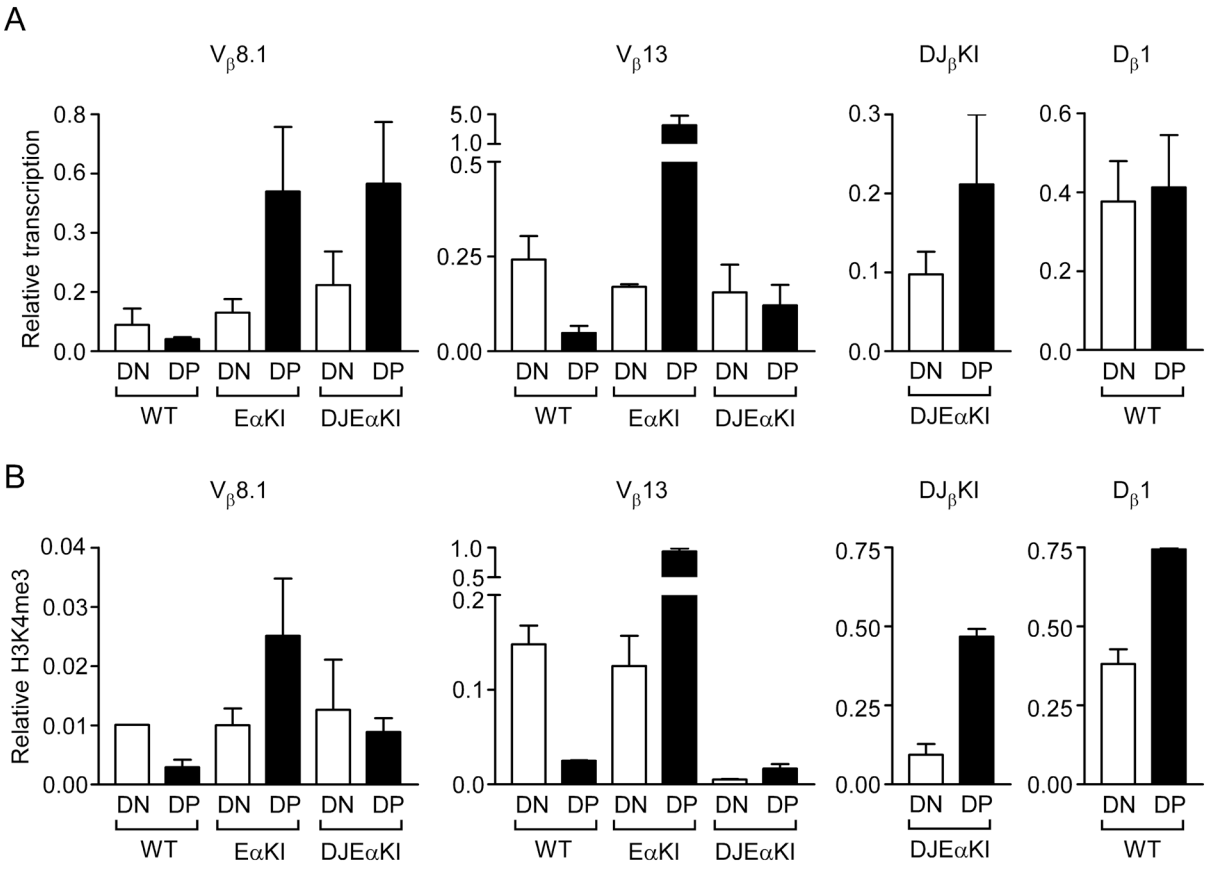

FIGURE 3.

Chromatin accessibility of DJEαKI alleles. (A) Germline transcription in wild-type (WT), EαKI and DJEαKI DN (all *Rag2*$^{-/-}$) and DP (all *Rag2*$^{-/-}$ x *Tcrb* tg) thymocytes, analyzed by quantitative real-time PCR. Results were normalized to those for *Actb* and represent the mean ± s.e.m. of 2–6 independent experiments, using cDNA diluted 1:10 for $D_\beta1$ and *Actb* PCRs and undiluted cDNA for $V_\beta13$ and $V_\beta8.1$ PCRs. (B) Chromatin immunoprecipitation of H3K4me3-modified nucleosomes of wild-type, EαKI and DJEαKI DN (all *Rag2*$^{-/-}$) and DP (all *Rag2*$^{-/-}$ x *Tcrb* tg) thymocytes. Ratios of bound to input were normalized to those for β_2–microglobulin (*B2m*) and represent the mean ± s.e.m. of 2–4 independent experiments.

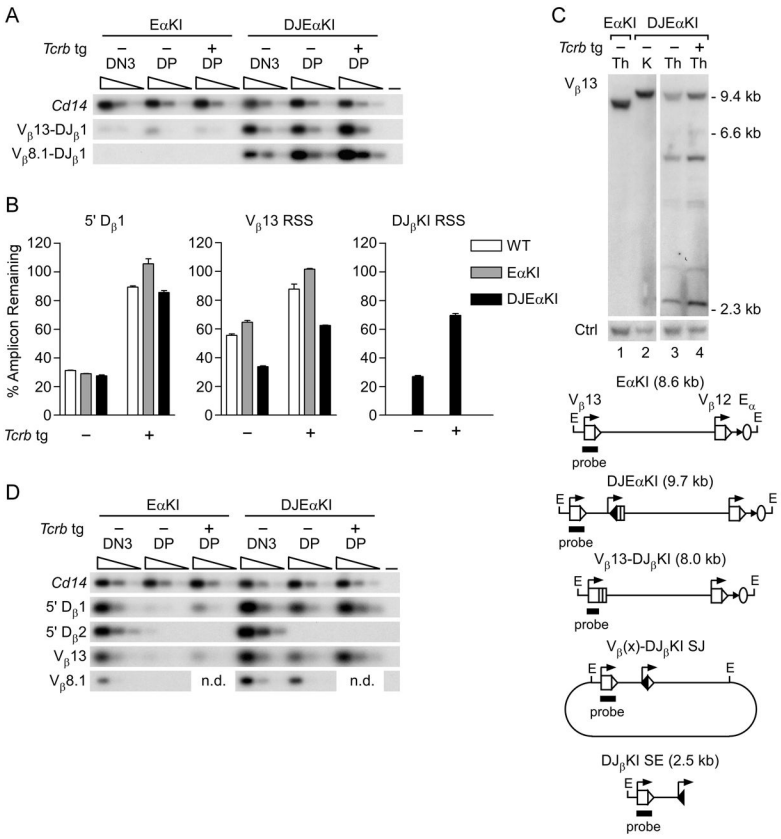

FIGURE 4.

Recombination of DJEαKI alleles. (A) Coding joint analysis. Genomic DNAs from sorted EαKI and DJEαKI DN3 and DP thymocytes without (−) or with (+) a *Tcrb* tg were serially three-fold diluted (wedges) and analyzed by PCR. Blots of PCRs using V_β and J_β1.1 primers were hybridized with a DJ_βKI-specific probe. *Cd14* amplification was used to control for DNA loading. –, no DNA. Data are representative of two independent experiments. (B) RSS usage. Genomic DNAs from DJEαKI kidney and from sorted wild-type (WT), EαKI and DJEαKI DP thymocytes, without (−) or with (+) a *Tcrb* tg, were analyzed by quantitative real-time PCR. Percent amplicon remaining was calculated as [(experimental amplicon in thymus/experimental amplicon in kidney)/(*B2m* in thymus/*B2m* in kidney)] x 100. Data are the mean ± s.e.m. of 2–3 samples for each genotype. (C) Genomic Southern blot. Top, unfractionated thymus (Th) and kidney (K) genomic DNAs were digested with *EcoR*I and analyzed by Southern blot using a V_β13 probe. DNA loading was assessed using a control (Ctrl) trypsinogen probe. Below, schematic of expected *EcoR*I fragments, including a diagram of predicted excision circles containing V_β(x)-DJ_βKI signal joint (SJ) recombination products. (D) SE analysis. Thymocyte genomic DNA samples were linker-ligated, serially three-fold diluted (wedges) and analyzed by PCR. *Cd14* amplification was used to control for DNA loading. –, no DNA. The data are representative of two independent experiments. n.d., not determined.

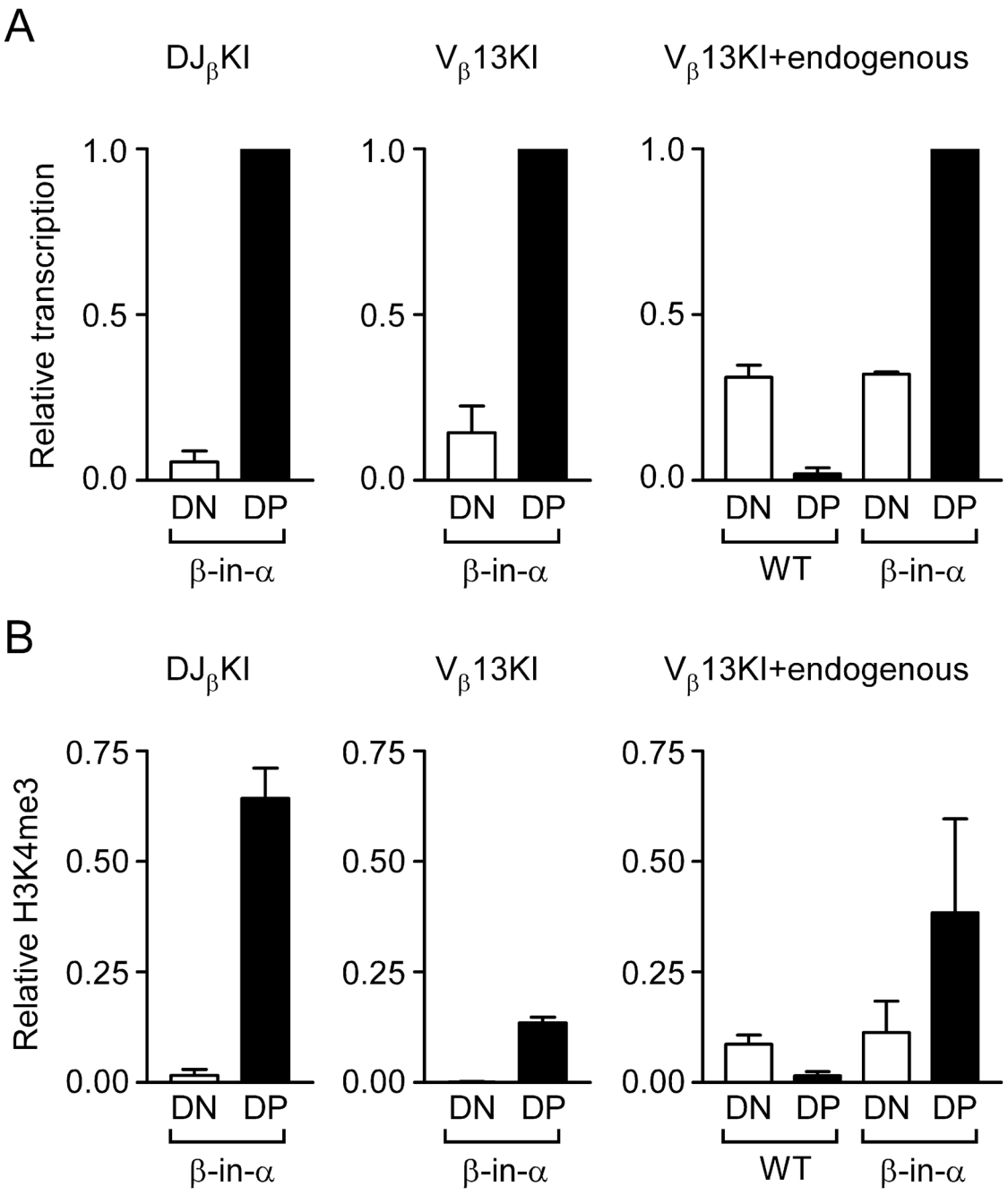

FIGURE 5.

Chromatin accessibility of β-in-α alleles. (A) Germline transcription in wild-type (WT) and β-in-α DN (*Rag2*$^{-/-}$) and DP (*Rag2*$^{-/-}$ x *Tcrb* tg) thymocytes was analyzed by quantitative real-time PCR. Data were normalized to *Actb* and then expressed as a fraction of the value inβ-in-α DP thymocytes. Results represent the mean ± s.e.m. of 2–4 independent experiments. (B) Chromatin immunoprecipitiation of H3K4me3-modified nucleosomes of wild-type (WT) and β-in-α DN (*Rag2*$^{-/-}$) and DP (*Rag2*$^{-/-}$ x *Tcrb* tg) thymocytes. Ratios of bound to input were normalized to those for *B2m* and represent the mean ± s.e.m. of 2–3 independent experiments.

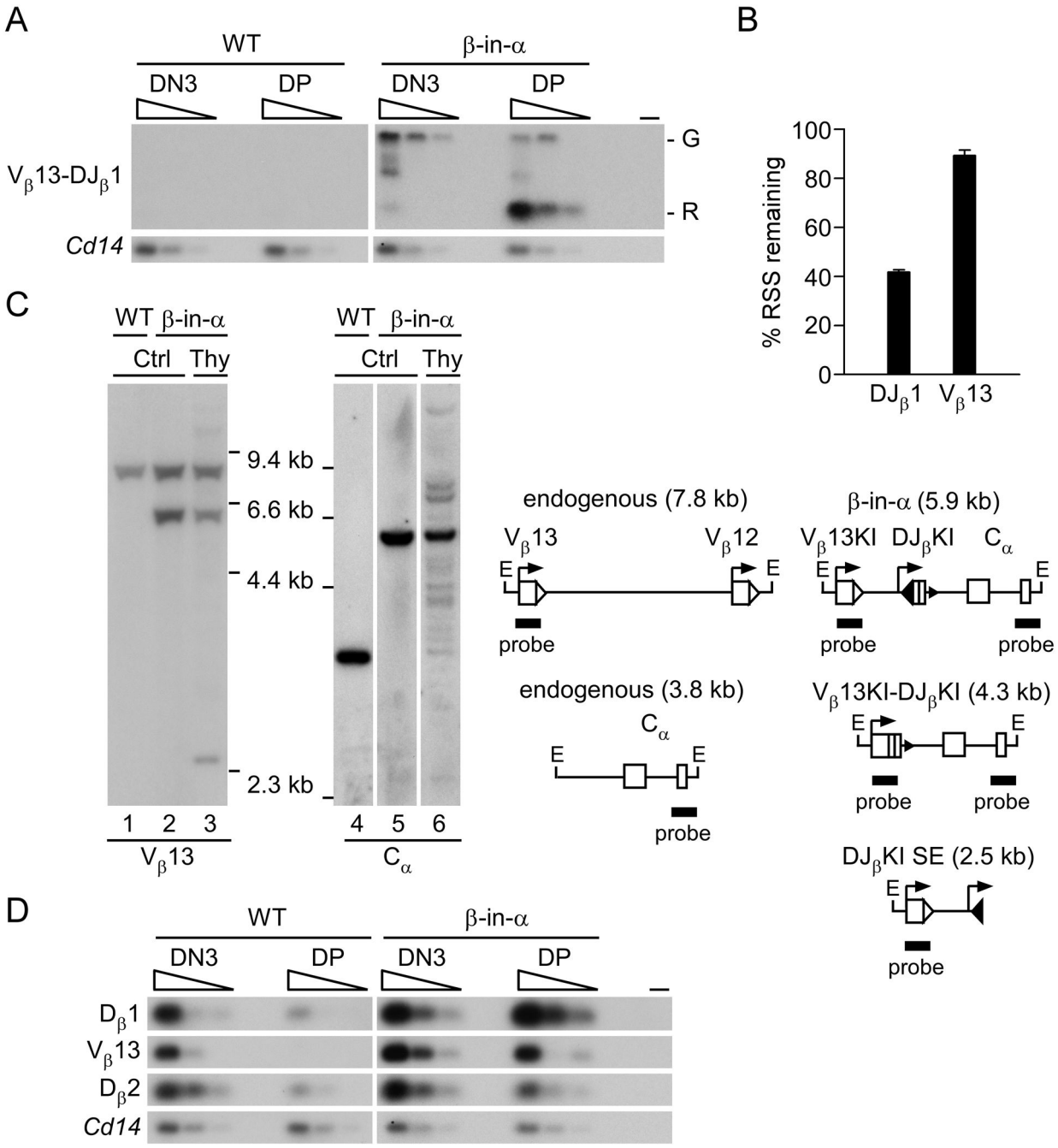

FIGURE 6.

Recombination of β-in-α alleles. (A) Coding joint analysis. Genomic DNAs from sorted wild-type (WT) and β-in-α DN3 and DP thymocytes were serially three-fold diluted (wedges) and analyzed by PCR. Blots of V_β to $J_\beta 1.1$ PCRs were hybridized with a DJ_βKI-specific probe. *Cd14* amplification was used to control for DNA loading. –, no DNA; G, germline $V_\beta 13$ KI-DJ_βKI; R, rearranged $V_\beta 13$KI-DJ_βKI. Data are representative of two independent experiments. (B) RSS usage. Genomic DNAs from β-in-α kidney and unfractionated thymus were analyzed by quantitative real-time PCR using DJ_βKI-and $V_\beta 13$KI-specific primers. Percent amplicon remaining was calculated as [(experimental amplicon in thymus/experimental amplicon in kidney)/(*B2m* in thymus/*B2m* in kidney)] x

100. Data are the mean ± s.e.m. of 2–3 samples. (C) Genomic Southern blot. Left, wild-type (WT) andβ-in-α nonrearranged control tissue (Ctrl) and β-in-α unfractionated thymus (Thy) genomic DNAs were digested with *EcoR*I and analyzed by Southern blot using $V_\beta 13$ or C_α probes. Right, schematic of expected *EcoR*I fragments. (D) SE analysis. Thymocyte genomic DNA samples were linker-ligated, serially three-fold diluted (wedges) and analyzed by PCR. *Cd14* amplification was used to control for DNA loading. $V_\beta 13$ primers amplify SEs from endogenous $V_\beta 13$ and $V_\beta 13$ KI. –, no DNA. The data are representative of three independent experiments.